J. Physiol. (1987), **385**, *pp.* 307–324
With 8 text-figures
Printed in Great Britain

ELECTRICAL CONSTANTS OF ARTERIALLY PERFUSED RABBIT PAPILLARY MUSCLE

BY A. G. KLÉBER AND C. B. RIEGGER

From the Department of Physiology, University of Berne, Buehlplatz 5, CH-3012 Berne, Switzerland

(*Received 16 June 1986*)

SUMMARY

1. Right ventricular rabbit papillary muscles were arterially perfused with a mixture of Tyrode solution, bovine erythrocytes, dextran and albumin. In the recording chamber, they were surrounded by a H_2O-saturated atmosphere of O_2 and CO_2 which served as an electrical insulator.

2. Conduction velocity and passive electrical properties were determined from intra- and extracellular potentials measured during excitation and during flow of subthreshold current.

3. The propagation of the action potential was linear along the muscle at a velocity of 55·6 cm/s. The extracellular wave-front voltage was 51·5 mV.

4. The following values for passive cable properties were obtained: (i) a ratio of extra- to intracellular longitudinal resistance of 1·2; (ii) an extracellular specific resistance (R_o) of 63 Ω cm; (iii) an intracellular specific resistance (R_i) of 166 Ω cm; (iv) a space constant λ of 0·357 mm; (v) a membrane time constant τ of 2·57 ms. The space constant λ^* recalculated for zero extracellular resistance was 0·528 mm.

5. Arresting perfusion with drop of perfusion pressure was associated with an immediate increase of the extracellular longitudinal resistance by 35 % and a decrease of conduction velocity by 13 %.

6. The present results demonstrate the important contribution of the extracellular resistance to electrotonic interaction and propagation in densely packed myocardial tissue. Moreover, changes in perfusion pressure are associated with changes in extracellular resistance, probably as a consequence of changes in intravascular volume.

INTRODUCTION

Cable properties of cardiac tissues have been analysed in various ways. Mostly, the spatial decay of membrane potential caused by point injection of current was used to measure electrotonic interaction in Purkinje fibres (Weidmann, 1952) and ventricular muscle (Tille, 1966). In tissues where the single cells are arranged to form a thin rod of syncytial tissue, such as Purkinje fibres, the decay of potential can be reasonably modelled with a linear electrical cable, except for the potential changes occurring close to the site of current injection (Matsuda, 1960; Pressler, 1984). Determination of cable properties in compact ventricular tissue is more difficult. Daut

(1982) examined the passive electrical properties of small guinea-pig papillary muscles by a voltage-clamp technique. This method allowed a direct measurement of the resistance and the capacitance of the membrane, whereas calculation of the longitudinal intracellular specific resistance depended on an assumption concerning the resistance of the extracellular space. Weidmann (1970) treated cylindrically shaped ventricular trabeculae as approximating a linear cable. He obtained cable constants from the combination of two experimental interventions: (i) the application of longitudinal extracellular current and (ii) the measurement of the extracellular bipolar electrogram during excitation. An advantage of Weidmann's method is that changes in the passive electrical properties can be related to changes in conduction velocity. The technique requires an electrical insulator (e.g. silicon oil, Weidmann, 1970) surrounding the preparation in order to avoid electrical shunting of the tissue's proper extracellular longitudinal resistance. At a boundary between densely packed ventricular tissue and a volume conductor, the wave-front of excitation is non-linear and one-dimensional cable theory is inadequate to describe the conditions for propagation (Suenson, 1985). In excised tissue a certain amount of extracellular shunt has to be accounted for because the tissue requires diffusional supply of oxygen and metabolic substrates from a superfusate.

In the present work cable properties, action potentials and conduction velocity were measured in an arterially perfused rabbit papillary muscle. In this preparation the metabolic demands are met by the arterial blood supply. This avoids electrical shunting by a superficial layer of fluid. The extracellular longitudinal resistance is entirely composed of elements situated in the relatively small volume between the densely packed myocardial cells. The results obtained in such an experimental model will be representative for the relationship between longitudinal impulse conduction and electrical properties in the ventricular wall. It allows the assessment of the effects of changes in the perfusion (e.g. ischaemia) and in the composition of the perfusate on electrical activity, extracellular resistance, cellular coupling and propagation. Moreover, the effect of drugs in the arterial fluid on cable properties and propagation can be studied without the need to account for diffusion gradients between the surface cell layers and the core of the muscle.

The results presented in this paper suggest that the relatively large resistance of the extracellular space has an important influence on the propagation velocity and on the magnitude of the extracellular field in compact ventricular tissue.

METHODS

Preparation

Rabbits weighing 2–3 kg were anaesthetized with an intravenous injection of pentobarbitone (50 mg/kg) and killed with a blow on the head. Formation of blood clots was prevented by intravenous administration of heparin (200 u/kg). The heart was rapidly excised and brought to a dissecting chamber. The great arteries, both atria and the orifices of the atrioventricular valves were removed from the ventricles with a single cut by a razor blade and the left-ventricular free wall was cut off with scissors. Afterwards, the preparation was pinned on a small Perspex plate covered with wax, the left side of the interventricular wall oriented downwards. The septal artery, which was easily visible in the cut section of the interventricular septum, was cannulated under a binocular microscope with a polyethylene tube tapered to a diameter of 100–200 μm. The delay between the removal of the heart from the animal and septal perfusion ranged from 4 to 6 min.

Following cannulation and perfusion, the free wall of the right ventricle and the non-perfused part of the interventricular septum were carefully removed. Finally, a preparation was positioned in the recording chamber which consisted of an arterially perfused part of the interventricular septum to which one to three papillary muscles were attached. Muscles were selected which showed no marked tapering at the apical end and inserted by a single tendon. The mean diameter of the muscles was $0{\cdot}95 \pm 0{\cdot}05$ mm ($\pm$S.E. of mean, $n = 20$), the mean cross sectional area $0{\cdot}75 \pm 0{\cdot}08$ mm^2 ($\pm$S.E. of mean, $n = 20$).

Perfusate

The perfusate (see Kléber, 1983) contained washed bovine erythrocytes (hematocrit 25%), albumin (2 g/l), dextran (molecular weight 70000; 40 g/l), insulin (1 u/l), heparin (400 u/l) and Tyrode solution of the following composition (mM): Na^+, 149; K^+, 4·5; Mg^{2+}, 0·49; Ca^{2+}, 1·8; Cl^-, 133; HCO_3^-, 25; $HPO_4^{2-} + H_2PO_4$, 0·4; and glucose, 20. The pH of the perfusion fluid was 7·35–7·40, the resistivity 81–85 Ω cm.

Perfusion

The perfusate was continuously stirred in a beaker to avoid sedimentation of erythrocytes. It was pumped at constant flow (roller pump, Ismatec, Switzerland) to a membrane oxygenator where it was equilibrated with O_2 and CO_2. The following elements were introduced into the flow line between the oxygenator and the recording chamber: (i) A conventional glass pH electrode, (ii) a droplet counter serving as flowmeter, (iii) a tap for interruption of perfusion, (iv) a filter (pore size 40 μm, Seidengazefabrik, Switzerland) and (v) a connexion to a pressure transducer (Statham, U.S.A.). The P_{CO_2} of the O_2–CO_2 mixture in the oxygenators was adjusted to yield a pH of 7·36–7·40 of the bicarbonate-containing perfusate (see below). The tubing passing from the oxygenators to the first tap and further to the recording chamber were made of stainless-steel in order to inhibit gas exchange between the perfusate and the surrounding atmosphere. Normally, the perfusion pressure was set to 40–45 mmHg by adjustment of the roller pump.

The recording chamber (made of Perspex) is shown on Fig. 1. The plate carrying the preparation was fixed to a transverse shaft and turned from a horizontal position to an angle of 30–40 deg. The tendon at the apex of the papillary muscle was attached to a platinum wire which was running through the hollow core of a cylindrical Perspex holder. This holder, which protruded into the recording chamber, was mounted on a micromanipulator at its base. It was used to position the papillary muscle, to adjust its resting length and it carried one of the electrodes through which extracellular current was applied. Connexions to the perfusion apparatus, to electrical ground, and a channel for suction of the venous effluent were placed in the posterior wall of the recording chamber. A mixture of 95% O_2 and 5% CO_2, saturated with H_2O, flowed into the chamber at the base through multiple holes drilled into the anterior and the side walls. The whole chamber was closed with a cover. An opening of $1{\cdot}0 \times 1{\cdot}0$ cm allowed access to the preparation for micro-electrodes. Temperature was maintained at 35 °C. Temperature control was achieved by warming the tubing with the perfusate and the gas mixture in a water-bath at constant temperature. In addition, the water from the thermostat was led through the partition of the double-walled cover of the recording chamber.

Recordings of extracellular and intracellular potentials

Intracellular floating micro-electrodes for the measurement of transmembrane potentials were pulled from borosilicate glass. d.c.-tip resistances were 15–20 MΩ when filled with 3 M-KCl. The tips (3–4 mm in length) were mounted on a fine AgCl-coated silver wire (diameter 50 μm). Extracellular electrodes were made by tungsten wire (Goodfellow Metals, diameter 30–50 μm).

Intracellular and extracellular recordings were obtained during application of a subthreshold d.c. pulse of 20 ms and an excitatory current pulse of double-threshold strength and 0·5–2 ms duration following with a delay of 20–30 ms. This pair of pulses was generated at a frequency of 75–100/min by a constant current source (Devices, U.K.). The current was applied longitudinally through the preparation between two large extracellular electrodes. One electrode was located at the apex of the papillary muscle the other electrode was a chlorided silver plate of 0·4 cm^2 surface area which was in contact with the left-ventricular side of the interventricular septum (Fig. 2) and electrically grounded. Current strength was measured by a feed-back amplifier introduced between the preparation and ground.

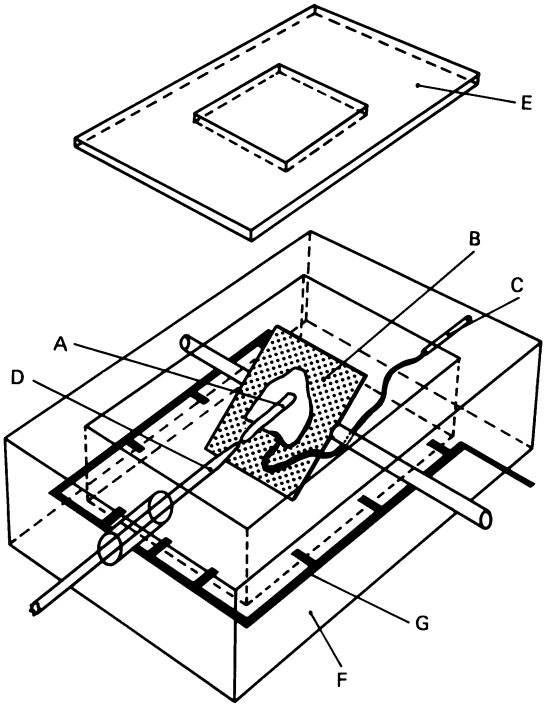

Fig. 1. Recording chamber: *A*, perfused rabbit interventricular septum with papillary muscle. *B*, wax-covered Perspex platform, mounted in an oblique position. *C*, connexion to perfusion apparatus. *D*, lever containing electrode, to which the tendon of the papillary muscle is fixed. *E*, double-walled cover of recording chamber with opening for recording electrodes. *F*, Perspex block forming the walls of the recording chamber which contain a canalicular system (G) through which the O_2/CO_2 mixture flows into the chamber. The connexion to ground and the suction for collecting venous blood are not shown.

For the registration of extracellular bipolar electrograms (see Fig. 2, upper part) and subthreshold voltage changes (Fig. 3) one extracellular electrode (corresponding to P_1 on Fig. 2) was moved with a micromanipulator along the fibre axis and a second extracellular electrode (corresponding to P_2 in Fig. 2) remained at a fixed position near to the base of the muscle. The distance Δx between the two electrodes was measured with the eyepiece micrometer of the binocular microscope at 25 × magnification. Transmembrane potentials were recorded between the intracellular floating electrode, usually located close to the apex of the papillary muscle, and the first extracellular electrode (P_3 and P_1 on Fig. 2*B*). Recording electrodes were connected to high-input impedance pre-amplifiers (Analog Device 515) and signals amplified by differential instrumentation amplifiers. The amplified traces representing current strength, extracellular and transmembrane potential were stored digitally in a signal memory recorder (Max Meyer Electronics, Switzerland). The data were analysed with a computer (Hewlett–Packard 9617) and displayed on a graphical plotter (HP 7470A). The paired *t* test was used for statistical comparison of values before and after interruption of perfusion (Table 3).

THEORY

The measurement of electrical constants from arterially perfused papillary muscle is based on the theoretical approach of Weidmann (1970) and on its modification by Wojtzcak (1979). In this theory, a cylindrically shaped trabecular muscle is treated

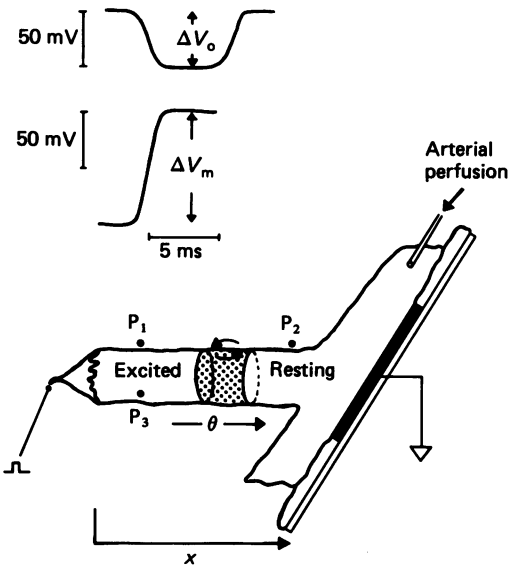

Fig. 2. Upper part: schematical presentation of the extracellular bipolar electrogram with amplitude ΔV_o, measured between points P_1 and P_2 and the transmembrane action potential with amplitude ΔV_m, measured between the intracellular site P_3 and P_1. Lower part: arterially perfused rabbit papillary muscle. The muscle is attached to the interventricular septum which contains the cannulated septal artery. The preparation is mounted on a wax-covered Perspex platform and connected to electrical ground via a chlorided silver plate. The tendon at the apex of the papillary muscle is fixed to a stainless-steel wire and lifted above the septum. Subthreshold and excitatory currents are applied between the apex (cathode) and base (anode), x corresponds to the distance from the apical end. The currents flow between the muscle's extra- and intracellular compartments, the surrounding atmosphere of the recording chamber being an electrical insulator. The central dotted segment indicates the zone of local current flow propagating at velocity θ.

as a one-dimensional electrical cable. It is exposed (i) to a subthreshold d.c. pulse flowing between two large extracellular electrodes and (ii) excited at one end. The justification of treating a perfused rabbit papillary muscle as a one-dimensional cable depends on several assumptions whose validity can be tested experimentally: (i) a constant shape (cylindrical or elliptical) of the muscle's cross-section, (ii) homogeneous distribution of extra- and intracellular resistivities along the cable axis and in the direction of the fibre radius and (iii) uniform propagation of the excitation wave-front after stimulation at one end. No potential gradients are allowed to exist between intracellular (or extracellular) sites situated within a given cross-sectional area and at a given time during excitation or flow of subthreshold current.

The theoretical changes of the extracellular bipolar electrogram and the membrane potential during excitation are shown in the upper part of Fig. 2. A schematical drawing of the arterially perfused papillary muscle is given in the lower part of Fig. 2. The extracellular electrogram corresponds to the voltage difference between points P_1 and P_2, membrane potential equals the voltage difference between P_3 and P_1. Fig. 2 depicts the excited and the resting segment of the fibre separated by the zone

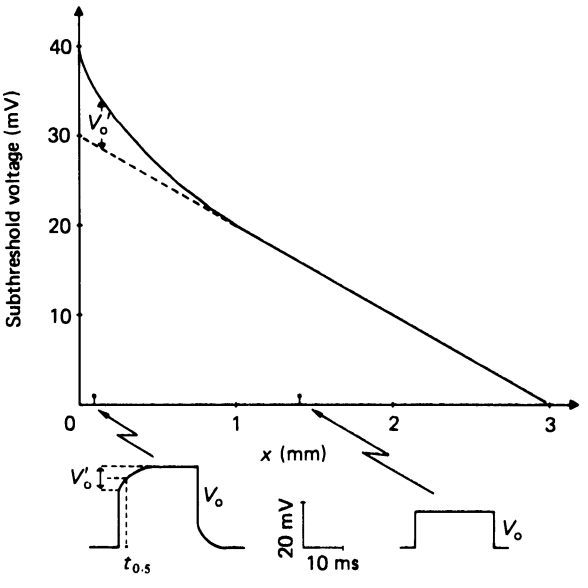

Fig. 3. Top: theoretical distribution of steady-state extracellular voltage along the fibre axis x during application of subthreshold current between apex and base (apex: $x = 0$ mm; base: $x = 3$ mm). Close to the apex of the muscle, the extracellularly applied current distributes between the extra- and intracellular space. This transmembrane current flow gives rise to deviation from linearity of the subthreshold voltage profile. Remote from the site of current injection the change of V_0 with x is linear. Bottom left: subthreshold voltage pulse close to the apex of the papillary muscle (0·1 mm). Transmembrane current flow produces a time-dependent voltage change V_0'. The space constant λ is obtained from the change of the steady-state value of V_0' with x, the membrane time constant τ is obtained from $t_{0.5}$ at a given x/λ. Bottom right: subthreshold voltage pulse remote ($> 5\lambda$) from the apical end. Note absence of time-dependent component.

of local current flow (wave-front) which has passed one half of the distance x. The medium around the fibre is an electrical insulator (for atmosphere in the recording chamber, see Methods). The rapid deflexion and inflexion on the bipolar extracellular electrogram indicate the passage of the wave-front under the electrodes. Thus, the velocity of propagation θ equals:

$$\theta = \frac{\Delta x}{t} \text{ (cm/s)}, \tag{1}$$

where Δx is the distance between the points P_1 and P_2 and conduction time t corresponds to the delay between the steepest part of the deflexion and inflexion on the bipolar electrogram.

From the same recordings, the ratio q of longitudinal extracellular (r_o) and intracellular (r_i) resistances can be calculated according to Weidmann (1970) and Wojtzcak (1979):

$$q = \frac{r_o}{r_i} = \frac{\Delta V_o}{\Delta V_m - \Delta V_o} \tag{2}$$

where ΔV_m is the amplitude of the transmembrane potential (absolute value) and ΔV_0 is the amplitude of the bipolar extracellular electrogram (absolute value).

Fig. 3 (top) shows the potential V_0 in the extracellular space resulting from current flow from the apex to the base of the papillary muscle. A subthreshold current pulse injected into the extracellular space at the end of the papillary muscle divides into current flowing through the extracellular resistance and current flowing through the cell membranes into the intracellular compartment. At a distance of several space constants λ from the apex, membrane current approaches zero, and consequently, extracellular voltage V_0 changes linearly along the x-axis. The longitudinal tissue resistance r_t, which consists of r_i and r_0 in parallel, is calculated from the slope of this linear portion and the current I (Weidmann, 1970):

$$r_t(\text{k}\Omega/\text{cm}) = \frac{1}{I}\frac{dV_0}{dx} = \frac{r_0 r_i}{r_0 + r_i}, \tag{3}$$

from eqns. (2) and (3), r_0 and r_i become:

$$r_0(\text{k}\Omega/\text{cm}) = \frac{1}{I}\frac{dV_0}{dx}(1+q), \tag{4}$$

$$r_i(\text{k}\Omega/\text{cm}) = \frac{1}{I}\frac{dV_0}{dx}\frac{(1+q)}{q}. \tag{5}$$

The specific intracellular (R_i) and extracellular (R_0) longitudinal resistances depend on the fraction of tissue volume occupied by the intra- and extracellular space respectively.

$$R_i(\Omega\ \text{cm}) = r_i\, A_i, \tag{6}$$

$$R_0(\Omega\ \text{cm}) = r_0\, A_0, \tag{7}$$

where A_i and A_0 correspond to the intra- and extracellular fraction of the cross-sectional area respectively.

The time constant τ (in ms) and the space constant λ (in mm) are obtained from V_0 measured close to the apex of the papillary muscle (Fig. 3, bottom trace). In this region, membrane current flowing through the capacitive elements after the onset of the current pulse produces a time-dependent change of the subthreshold voltage (V_0', Fig. 3, bottom trace). At a given distance from the end of the muscle, the time $t_{0.5}$, measured at half-amplitude (0·5 V_0') of the time-dependent change V_0' (see Fig. 3), is related to τ by:

$$\tau = \frac{t_{0.5}}{X/2 + 0.25}, \tag{8}$$

where X is the normalized distance from the end x/λ (Weidmann, 1970; Jack, Noble & Tsien, 1975). Close to the apex of the papillary muscle, an exponential decay of the voltage V_0' is superimposed on the linear voltage change (Weidmann, 1970). The space constant λ can be read directly from a semilogarithmic plot of V_0' *versus* x, where it corresponds to the distance over which an e-fold change of V_0' is observed.

The specific membrane resistance (R_m) and capacitance (C_m) are obtained from λ, τ, r_0, r_i and an estimate of the membrane surface through which the electrotonic current is flowing (Weidmann, 1970).

RESULTS

Propagation along the papillary muscle

The homogeneity of longitudinal propagation was tested by measuring multiple conduction times between the fixed basal extracellular electrode and the apical extracellular electrode placed at different locations along the muscle. Fig. 4 gives the relationship between conduction time and interelectrode distance from a single

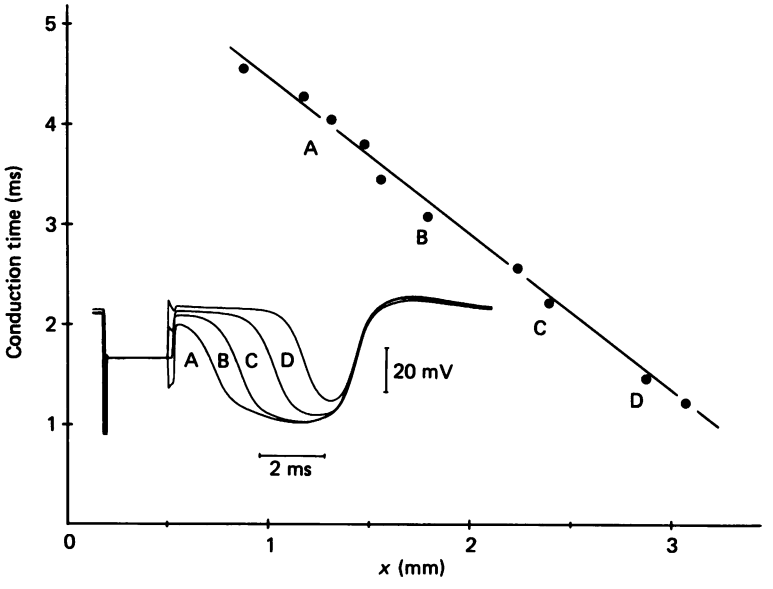

Fig. 4. Propagation of the action potential along the fibre. Abscissa: distance along the fibre axis, $x = 0$ refers to the apical end. Ordinate: conduction time between apical and basal electrode. Dots represent sequential measurements obtained from bipolar extracellular electrograms in a single experiment whereby the apical electrode is moved towards the electrode at the base of the muscle. The straight line is fitted to the individual measurements by linear regression (correlation coefficient $r = 0{\cdot}991$). The conduction velocity calculated from the line is 64 cm/s. Bipolar electrograms taken at points A to D are shown in the inset (muscle No. 12.3.86.2).

experiment. The individual measurements were taken during a time period of about 2 min. Normally, the deflexion on the bipolar extracellular electrogram was clearly distinguishable from the stimulus artifact at distances $> 0{\cdot}8$ mm from the end of the muscle. The straight line was fitted to the points by linear regression (regression coefficient $r = 0{\cdot}990$). In seventeen experiments, the mean of the regression coefficient was 0·989 ($\pm 0{\cdot}011$ S.D.; range 0·962–0·998) indicating a very consistent linear propagation in the longitudinal direction. The velocity of propagation was obtained from the linear curve in seventeen preparations and from single measurements of activation times in three preparations. The mean value was 55·6 cm/s (Table 1).

TABLE 1. Conduction velocity and characteristics of intra- and extracellular potentials of arterially perfused rabbit papillary muscle

	θ (cm/s)	ΔV_m (mV)	$\dot{V}_{m,max}$ (V/s)	ΔV_o (mV)	$\dot{V}_{o,min}$ (V/s)	$\dot{V}_{o,max}$ (V/s)
n	20	20	14	20	14	14
Mean	55·6	98·7	130·9	51·5	−65·7	67·9
± S.E. of mean	2·3	1·6	12·9	2·6	8·4	5·9

θ, longitudinal conduction velocity. ΔV_m, amplitude of transmembrane action potential. $\dot{V}_{m,max}$, maximal upstroke velocity of transmembrane action potential. ΔV_o, amplitude of extracellular bipolar electrogram. $\dot{V}_{o,min}$, minimal velocity of deflexion of extracellular bipolar electrogram. $\dot{V}_{o,max}$, maximal velocity of inflexion of extracellular bipolar electrogram.

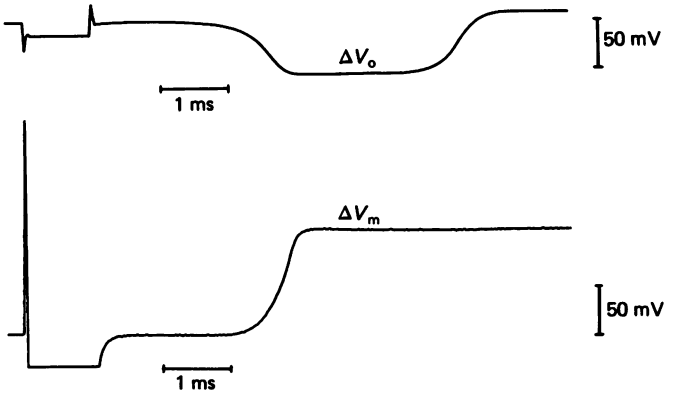

Fig. 5. Bipolar extracellular electrogram (top trace) and initial portion of the transmembrane action potential (bottom trace). The ratio $r_o/r_i = 1{\cdot}08$ is calculated from the amplitudes $\Delta V_o = 56$ mV and $\Delta V_m = 108$ mV (muscle No. 6.11.85.2). The lower portion of the stimulus artifact on the botton trace is cut off.

Transmembrane action potentials and extracellular electrograms

Transmembrane action potentials measured with floating micro-electrodes had a mean amplitude of 98·7 mV (Table 1). This value is significantly lower than values measured with the same technique in Langendorff-perfused guinea-pig ventricles (personal observation) but close to the results obtained in isolated rabbit ventricular tissue (Johnson & Tille, 1961).

A simultaneous recording of the early part of the transmembrane action potential and the bipolar extracellular electrogram is illustrated in Fig. 5. The extracellular electrograms showed a distinct plateau at an interelectrode distance of 1–1·5 mm or more. The presence of a plateau in the extracellular electrogram is a necessary condition to allow the ratio r_o/r_i to be calculated from ΔV_m and ΔV_o (Wojtzcak, 1979). It indicates that the wave-front of excitation has passed the apical electrode and has left the apical segment fully depolarized before producing local current under the basal electrode. At a given interelectrode distance, the duration of the plateau of the extracellular electrogram depends on the conduction velocity θ and the slope of the deflexion and inflexion. The mean minimal steepness (deflexion, $\dot{V}_{o\,min}$) of the

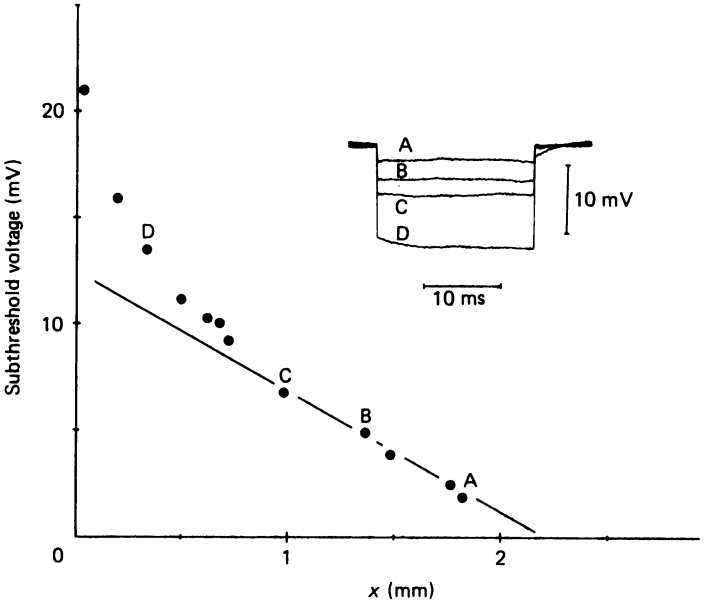

Fig. 6. Distribution of extracellular voltage V_0 after application of a subthreshold constant-current pulse ($I = 5{\cdot}3\ \mu A$) of 20 ms duration. V_0 is measured between a fixed basal electrode located at $x = 2{\cdot}25$ mm from the apical end ($x = 0$) and an electrode which is moved from the apex to the base. The straight line is fitted to the points at $x > 1$ mm by linear regression ($r = 0{\cdot}992$). Close to the apex, transmembrane current flow produces a deviation of V_0 from linearity. Subthreshold voltage pulses A to D shown in the inset were recorded with apical electrode situated at 1·82, 1·36, 0·99 and 0·34 mm from the apical end (muscle No. 6.11.82.3).

wave-front in the extracellular electrogram was −65·7 V/s, the mean maximal steepness 67·9 V/s (inflexion, $\dot{V}_{0,\max}$), for a mean amplitude ΔV_0 of 51·5 mV (Table 1). These values were in close proportion to the mean maximal upstroke velocity of the transmembrane action potential of 130·9 V/s and the mean amplitude ΔV_m of 98·7 mV (Table 1). They suggest that the shape of the wave-front (close to both extracellular electrodes) did not markedly deviate from a plane sheet oriented perpendicular to the fibre axis (see Discussion).

The ratio of the extracellular to the intracellular longitudinal resistance r_o/r_i, obtained from ΔV_m and ΔV_0, was 1·08 in the experiment illustrated in Fig. 5. The mean value of r_o/r_i from twenty different muscles was 1·2 (Table 2).

Extracellular voltage distribution after application of subthreshold current

Fig. 6 illustrates the distribution of the extracellular voltage along the papillary muscle after application of a subthreshold current pulse of 5·3 μA current strength and 20 ms duration. In sixteen experiments, the longitudinal tissue resistivity r_t was obtained from the linear curve which was fitted to the points remote from the apical end. For the linear curve fit, those voltage signals were taken which showed no distinct time-dependent component (signals A–C in Fig. 6). Usually, these points were located at greater than three space constants distance from the apical end. The mean

TABLE 2. Cable properties of arterially perfused papillary muscle

	r_o/r_i	R_t (Ω cm)	R_o (Ω cm)	R_i (Ω cm)	λ (mm)	λ^* (mm)	τ (ms)	R_m (kΩ cm²)	R_m^* (kΩ cm²)	C_m (μF/cm²)
n	20	19	19	19	9	9	9	9	9	9
Mean	1·2	116	63	166	0·357	0·528	2·57	1·25	2·57	2·49
±S.E. of mean	0·1	7	5	11	0·038	0·056	0·20	0·26	0·20	0·41

r_o/r_i, ratio of extra- to intracellular longitudinal resistance. R_t, specific longitudinal resistance of whole papillary muscle. R_o, extracellular specific resistance. R_i, intracellular specific resistance. λ, space constant. λ^*, space constant, recalculated for zero extracellular resistance. τ, time constant. R_m, specific membrane resistance. R_m^*, specific membrane resistance, calculated from τ and a C_m of 1 μF/cm². C_m, specific membrane capacitance. R_o and R_i are calculated on the base of an extra- to intracellular space ratio of 1 : 3 (Polimeni, 1974).

regression coefficient obtained from sixteen different muscles, was 0·982 (±0·049 S.D.; range 0·801–0·999). In the remaining three experiments r_t was calculated from a single measurement of a subthreshold voltage pulse. For comparison, the values of r_t were normalized with the fibre's cross-sectional area A and expressed as specific longitudinal tissue resistivity R_t (in Ω cm), where $R_t = r_t A$. The mean R_t from nineteen different muscles amounted to 116 Ω cm (Table 2). The values of the specific intracellular and extracellular longitudinal resistivities (R_i, mean 166 Ω cm; R_o, mean 63 Ω cm; Table 2) were calculated for each experiment from the ratio r_o/r_i, r_t and an assumed extracellular to intracellular space ratio of 1 : 3 (Polimeni, 1974).

For the determination of the space constant λ and the membrane time constant τ (nine experiments), seven to nine measurements of V_0 were made in the non-linear part of the subthreshold voltage profile, as illustrated in Fig. 6. For each of these points the non-linear component V_0' of the subthreshold voltage was obtained by subtraction of the linear portion (determined by linear correlation) from the steady-state value of V_0. The semilogarithmic plot of $\ln V_0'$ *versus* x is shown in Fig. 7 from the same experiment as illustrated in Fig. 6. The straight line was fitted to the points by linear regression, with a regression coefficient $r = 0{\cdot}972$. In all nine experiments the values could be reasonably well fitted with a linear curve (mean $r = 0{\cdot}927$, ±0·100 S.D., range 0·701–0·999). This indicates that the decay of V_0' which is attributed to transmembrane current can be represented by a single exponential. The mean of the space constant λ calculated from the linear curve fit in each experiment was 0·357 mm (Table 2). The space constant λ^* (mean = 0·528 mm, Table 2) corresponding to the constant of electrotonic decay in a infinite volume conductor ($r_o = 0$) was obtained from $(\lambda^*)^2 = \lambda^2(1 + r_o/r_i)$.

The membrane time constant was calculated from the time $t_{0{\cdot}5}$ measured at half of the amplitude of time-dependent extracellular voltage change V_0'. The simple relationship $\tau = t_{0{\cdot}5}/X + 0{\cdot}25$ is an approximation which gets close to the true value of τ at distances further than approximately 1·3 space constants from the site of current injection (Jack, Noble & Tsien, 1975). Fig. 8 depicts the change of the subthreshold voltage V_0 with the time-dependent component V_0' for measuring sites situated at 1·55 and 2·03 space constants ($X = 1{\cdot}55$ and 2·03 respectively) from the apical end. The values obtained for τ were 3·14 and 3·27 ms respectively. The mean value for τ from nine different muscles was 2·57 ms (Table 2).

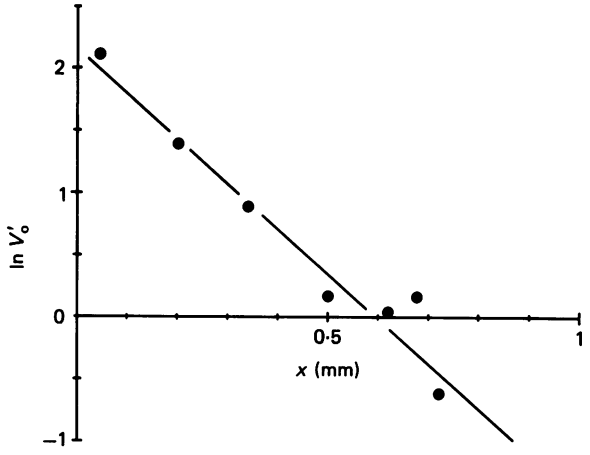

Fig. 7. Semilogarithmic plot of non-linear component of extracellular voltage drop V_o' from the experiment shown in Fig. 6. Ordinate: ln V_o'. Abscissa: distance x from apical end. Straight line is superimposed by linear regression ($r = 0{\cdot}975$), showing that the non-linear component can be represented by a single exponential decay. Space constant $\lambda = 0{\cdot}31$ mm.

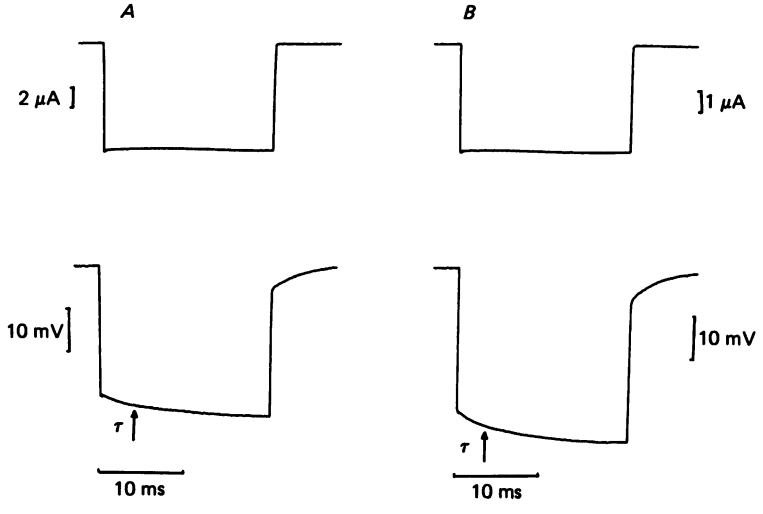

Fig. 8. Subthreshold current (top traces) and extracellular voltage steps (bottom traces). The voltage steps are measured between a fixed electrode at the base and an apical electrode which is positioned at 2·03 space constants (A) and at 1·55 space constants (B) from the apical end. The membrane time constant obtained from measuring $t_{0\cdot5}$ (see Theory) is 3·14 ms in A and 3·27 ms in B (muscle No. 15.2.86).

Computation of the specific membrane resistance and specific membrane capacitance requires an assumption concerning the membrane surface area through which the electrotonic current is flowing. The simplest model representing the rather complex cellular architecture (Sommer, 1979) consists of cylindrical cellular elements of identical diameter running in parallel to the fibre axis. The membrane surface area

TABLE 3. Effect of drop of perfusion pressure on extracellular electrogram, conduction velocity and longitudinal resistances (changes in percentages)

	ΔV_o	θ	r_o/r_i	r_o	r_i
n	10	10	10	10	10
Mean	+8*	−13*	+18*	+35*	+14*
±S.E. of mean	2	5	4	8	4

* Denotes statistical significance ($P < 0.05$).

can be calculated from the measured macroscopic fibre diameter, an assumed extra- to intracellular space ratio (1 : 3, Polimeni, 1974) and an average assumed diameter of the cellular element (15 μm, Sommer, 1979). Table 2 gives two different values for the specific membrane resistance, R_m and R_m^*. The first, R_m (mean value = 1·25 kΩ cm^2), was calculated on the basis of the above assumptions about cell membrane surface, from λ, r_i and r_o. The value R_m^* (mean = 2·57 kΩ cm^2) was obtained from the time constant τ and an assumed value for the specific membrane capacitance of 1 μF/cm^2 which is thought to be generally valid for most biological membranes (e.g. Cole, 1968). The calculated mean value for the specific membrane capacitance (from τ and R_m) was 2·49 μF/cm^2, i.e. more than twice the assumed value (Table 2). This may indicate that R_m underestimated the real value of specific membrane resistance.

Immediate effects of perfusional arrest on conduction velocity and longitudinal resistances

In order to assess the effect of the arterial perfusion on conduction velocity and the longitudinal tissue resistances, the changes of θ, r_t, r_o and r_i were measured between 15 to 60 s after complete interruption of arterial perfusion (ten experiments, Table 3). In the first 60 s no major electrical changes are to be expected from ischaemic metabolism (e.g. Kléber, 1983). Moreover, the high oxygen content (96 %) of the atmosphere in the recording chamber prevented a fall of P_{O_2} in the muscle below a critical level. Therefore, the observed changes are likely to reflect solely effects of perfusional arrest such as drop of perfusion pressure and a decrease in intravascular volume. The drop of perfusion pressure produced a small but significant decrease of conduction velocity of 13 % (Table 3). This decrease was associated with an increase of the extracellular longitudinal resistance of 35 % and an increase of intracellular longitudinal resistance of 14 %. Both changes were significant. The substantial increase of the extracellular resistance was also reflected in an increase of the amplitude of the extracellular electrogram by 8 %.

DISCUSSION

Longitudinal conduction

Our value for conduction velocity (55·6 cm/s) is in close accordance to measurements obtained in isolated superfused ventricular tissue (50 cm/s; Spach, Miller, Geselowitz, Barr, Kootsey & Johnson, 1981) and in subepicardial layers of whole Langendorff-perfused hearts (50 cm/s; Kléber, Janse, Wilms-Schopmann, Wilde & Coronel, 1986). The linear conduction profile (Fig. 5) indicated that superficial

propagation in apico-basal direction was homogeneous over the whole bundle. This argues against an involvement of the specific ventricular conducting system which overlies the base of the papillary muscles in dog (Matsuda, 1960; Veenstra, Joyner & Rawling, 1984).

A non-planar shape of the propagating wave-front is found in the presence of an extracellular volume conductor surrounding the preparation (Suenson, 1985). In this case, the lower extracellular resistance of the superficial tissue layers produces an increase of θ and a curved radial velocity profile. The curved form of the wave-front is associated with a reduction of the steepness of the wave-front, i.e. a decrease in the maximal upstroke velocity of the superficial transmembrane action potential (Suenson, 1985). In the present experimental arrangement, the fibre was in contact with an electrical insulator (H_2O-saturated atmosphere of the recording chamber). This does not however exclude some low-resistance shunting by the small subendocardial connective tissue layer surrounding the tightly packed ventricular fibres (Sommer & Scherer, 1985). Our results suggest that such resistive inhomogeneities within the bundle had no major distorting effect on the propagating wave-front. The steepness of the wave-front at the surface (derived from the minimal and maximal rates of change of V_0 relative to ΔV_0, Table 1) was virtually the same as the steepness at an estimated depth of 100–150 μm (derived from the maximal upstroke velocity of the transmembrane action potential relative to its amplitude ΔV_m, Table 1). This is the depth of penetration of floating micro-electrodes determined morphologically (Janse, Tranum-Jensen, Kléber & van Capelle, 1978; Tranum-Jensen & Janse, 1982).

Passive cable properties

The ratio of extracellular to intracellular resistance as calculated from the amplitudes of the transmembrane action potential and the extracellular electrogram was 1·2, i.e. significantly higher than 0·33 (Weidmann, 1970), 0·33 (Clerc, 1976) and 0·60 (Wojtzcak, 1979, his Fig. 3). This difference is due predominantly to the larger amplitude of the extracellular electrogram in our experiments, whereas the amplitude of the transmembrane action potentials compares favourably to other measurements (rabbit papillary muscle, Johnson & Tille, 1961; cow ventricle, Wojtczak, 1979). The extracellular voltage across the longitudinal wave-front was approximately 20 mV in Weidmann's (1970) and Clerc's (1976) experiments, whereas our value (51·5 mV) was more than 2-fold larger and close to the wave-front voltage reported from measurements in whole hearts *in situ* (closed-chest dog, ΔV_0 = 58–65 mV, Vander Ark & Reynolds, 1970; open-chest dog, ΔV_0 = 46 mV. Roberts, Hersch & Scher, 1979). This suggests that the small (20 μm) layer of Tyrode solution around the fibre used for nutritional supply may have partially shunted the superficial extracellular resistance in the experiments which were based on the superfusion technique of Weidmann (1970). Further evidence for a large magnitude (50 mV or more) of the extracellular wave-front voltage in ventricular myocardial tissue is provided by the amplitudes of cardiac-injury action potentials which can be regarded as equivalent to ΔV_0, i.e. to the extracellular potential difference between an unexcited and an excited region. Acute ischaemic injury produced extracellular potentials of a total amplitude of about 50 mV (perfused pig heart, Kléber, Janse, van Capelle & Durrer, 1978); acute mechanical injury was associated with extracellular potentials of an

amplitude of 50 mV in turtle heart and of 75 mV in dog heart (Eyster & Gibson, 1947).

In addition to the determination of r_o/r_i, the absolute values for extra- and intracellular longitudinal specific resistance, R_o and R_i, were obtained from the independent measurement of longitudinal tissue resistance r_t. The consistent linearity of the extracellular voltage profile remote from the site of current injection (Fig. 5) was a necessary condition for the application of the linear-cable theory (see Theory section or Weidmann, 1970). Our value for the specific longitudinal tissue resistivity R_t was 116 Ω cm. It compares to 152 Ω cm (Weidmann, 1970) and 125 Ω cm (calculated from Clerc, 1976) obtained from isolated subendocardial ventricular fibres and to 225 Ω cm (Rush, Abildskov & McFee, 1963) and 199 Ω cm (Roberts *et al.* 1979) obtained from subepicardial layers of open-chest dog hearts. The reason for the higher values measured in the subepicardium is not entirely evident. In the case of epicardial determinations, only part of the subthreshold current applied to measure R_t will flow parallel to the longitudinal axis of the fibre, because fibre orientation changes with increasing depth of the ventricular wall. This is likely to cause an over-estimation of R_t (Roberts *et al.* 1979).

Extracellular resistivity (mean $R_o = 63$ Ω cm) calculated on the basis of a 1 : 3 extra- to intracellular space ratio (Polimeni, 1974) was somewhat higher than the resistivity of Tyrode solution (51 Ω cm; Weidmann, 1970) but lower than the resistivity of the erythrocyte-containing perfusate (81–85 Ω cm). This may be taken to indicate that the resistivity of blood contributes to R_o and to the magnitude of the extracellular field in blood-perfused hearts. The mean specific resistance of the intracellular space (R_i) was 166 Ω cm. This is significantly lower than the values obtained by Weidmann (1970) in sheep ventricular bundles (470 Ω cm), but in good agreement with R_i measured in ventricular muscle with $^{42}K^+$ diffusion (240 Ω cm, Weidmann, 1966) and with R_i measured in ungulate Purkinje fibres (181 Ω cm, Weidmann, 1952). More recently, Daut (1980) estimated R_i in guinea-pig ventricle to be 200–250 Ω cm. This estimate included some uncertainty about the assumed ratio r_o/r_i. The value for R_i would become lower with increasing r_o (195 Ω cm at $r_o/r_i = 1:3$).

Our value obtained for the space constant λ was 0·357 mm. This is lower than most values measured in isolated, superfused tissue (0·100–0·300 mm, Tille, 1966; 0·880 mm, Weidmann, 1970; 0·650 mm, McGuigan, 1974; 0·580 mm, Daut, 1982). The large resistance of the extracellular space is likely to account for this difference. Recalculation for the case of an infinite-volume conductor (zero extracellular resistance) yielded a λ of 0·528 mm (Table 1). A second factor which influences the space constant is resting membrane resistance which depends on the extracellular K^+ concentration. Daut obtained a space constant of 0·580 mm for a $[K^+]_o$ of 3 mM and of 0·500 mm for a $[K^+]_o$ of 5·4 mM which is close to our value at $r_o = 0$ and $[K^+]_o$ of 4·5 mM. The mean value obtained for the membrane time constant $\tau = 2{\cdot}57$ ms compares to 6·6 ms (Daut, 1982) and to 4·4 ms (Weidmann, 1970). Whereas the difference between Daut's and Weidmann's data may be explained by the different $[K^+]_o$, the reason for our low value of τ is not completely evident. Partially, it may be related to the limitations of our method: (i) the determination of the take-off point of the time-dependent subthreshold voltage V'_o (Fig. 8) was relatively inaccurate,

(ii) the calculation of τ from $t_{0.5}$ depended on the accurate measurement of the distance x between the apical end and the recording electrode, and (iii) the time constant was obtained from one to two single measurements in each experiment. These eventual experimental restrictions do not apply to the determination of the other cable constants which were (with exception of r_o/r_i) determined from linear curve fits and independent from the absolute value of x.

As extensively discussed by others (Weidmann, 1970; Daut, 1982), calculation of the specific membrane resistance R_m involves assumptions about the fraction of the cell membrane surface which is crossed by the subthreshold electrotonic current. A test for the validity of these assumptions is usually made by calculating the specific membrane capacitance from R_m and the membrane time constant, because a value $C_m = 1\ \mu F/cm^2$ is assumed to be representative for most biological membranes (Cole, 1968). Our results suggest that R_m as calculated from λ, r_o, r_i and the assumed fibre dimensions was underestimated in the present experiments. Even with setting C_m to 1 $\mu F/cm^2$ and calculating R_m from C_m and τ, the value of R_m (2·57 kΩ cm^2) was by a factor of two lower than the values for specific membrane resistance reported by Dant (1982). This difference reflects the significantly smaller value for the membrane time constant in the present experiments, as discussed above.

Immediate effects of arresting perfusion

One of the major purposes of this investigation was to develop a method for assessing the effect of arterial perfusion on conduction velocity and cable properties. As indicated by the magnitude of the extracellular electrogram, and the ratio r_o/r_i, the extracellular resistance is an important determinant of electrotonic interaction and propagation in blood perfused ventricular tissue. In our analysis of electrical constants the extracellular space was represented by a single resistor. This is certainly an oversimplification, because the intravascular space containing the perfusate is likely to have a different resistance than the interstitial space. Depending on the perfusion conditions, the intravascular space may occupy 54–84 % of the extracellular volume (van den Bos & de Jang-Strakova, 1982). Therefore, it is likely that changes of the composition of the perfusate or of the perfusion pressure have a significant effect on the gross extracellular electrical resistance. It is known that the normal perfusion pressure in the dense myocardial capillary tree is also an important determinant of the mechanical behaviour. Arrest of perfusion causes an immediate loss of the 'erectile' effect (or so-called hydrolic stiffness) on the myocardium, i.e. a decrease of the diastolic stiffness and the developed tension (Vogel, Apstein, Briggs, Gaasch & Ahn, 1982). In the present study, arrest of perfusion was associated with an expected marked increase of the extracellular longitudinal resistance by 35 % and a decrease of the conduction velocity by 13 %. Astonishingly, the internal longitudinal resistance increased by a small (14 %) but significant amount as well. The reason for this change is not clear. It may be speculated whether it is related to the loss of the hydrolic stiffness of the capillary tree. The diminution of the extracellular volume may turn the average orientation of the cells and, thereby, increase the number of resistive intracellular elements in longitudinal direction.

In conclusion, our results indicate that the resistance of the extracellular space contributes markedly to the passive electrical properties of myocardial tissue. It

explains the high amplitude of the extracellular wave-front voltage and, therefore, it will largely influence the amplitude of the electrocardiogram. The space constant in the ventricular wall is likely to be significantly shorter than in tissue layers located adjacent to a volume conductor (e.g. intracavitary fluid). Moreover, the extracellular resistance of the whole heart is sensitive to changes in perfusion pressure, probably because of concomitant changes in intravascular volume.

We would like to express our gratitude to Professor J. A. S. McGuigan for help with the manuscript and to Mrs Keller, Mr Cigada and Mr de Limoges for technical assistance. This work was supported by the Swiss National Science Foundation (grant 3.958–0.82 to A.G.K.) and by the Swiss Foundation of Cardiology.

REFERENCES

CLERC, L. (1976). Directional differences of impulse spread in trabecular muscle from mammalian heart. *Journal of Physiology* **255**, 335–346.

COLE, K. S. (1968). *Membranes, Ions and Impulses*. Berkeley and Los Angeles: University of California Press.

DAUT, J. (1982). The passive electrical properties of guinea-pig ventricular muscle as examined with a voltage clamp technique. *Journal of Physiology* **330**, 221–242.

EYSTER, J. A. E. & GIBSON, W. E. (1947). Electrical characteristics of injuries to heart muscle. *American Journal of Physiology* **150**, 573–579.

JACK, J. J. B., NOBLE, D. & TSIEN, R. W. (1975). *Electrical Current Flow in Excitable Cells*. Oxford: Clarendon Press.

JANSE, M. J., TRANUM-JENSEN, J., KLÉBER, A. G. & VAN CAPELLE, F. J. L. (1978). Techniques and problems in correlating cellular electrophysiology and morphology in cardiac nodal tissues. In *The Sinus Node, Structure, Function and Clinical Relevance*, ed. BONKE, F. I. M., pp. 183–194. The Hague, Boston, London: Martinus Nijhoff Medical Division.

JOHNSON, E. A. & TILLE, J. (1961). Investigations of the electrical properties of cardiac muscle fibers with the aid of intracellular double-barrelled electrodes. *Journal of General Physiology* **44**, 443–467.

KLÉBER, A. G., (1983). Resting membrane potential, extracellular potassium activity, and intracellular sodium activity during acute global ischemia in isolated perfused guinea pig hearts. *Circulation Research* **52**, 442–450.

KLÉBER, A. G., JANSE, M. J., VAN CAPELLE, F. J. L. & DURRER, D. (1978). Mechanism and time course of S–T and T–Q segment changes during acute regional myocardial ischemia in the pig heart determined by extracellular and intracellular recordings. *Circulation Research* **42**, 603–613.

KLÉBER, A. G., JANSE, M. J., WILMS-SCHOPMAN, F. J. G., WILDE, A. A. M. & CORONEL, R. (1986). Changes in conduction velocity during acute ischemia in ventricular myocardium of the isolated porcine heart. *Circulation* **73**, 189–198.

MCGUIGAN, J. A. S. (1974). Some limitations of the double sucrose gap, and its use in a study of the slow inward current in mammalian ventricular muscle. With an Appendix by MCGUIGAN, J. A. S. & TSIEN, R. W. *Journal of Physiology* **240**, 775–806.

MATSUDA, K. (1960). Some electrophysiological properties of terminal Purkinje fibres of heart. In *Electrical Activity of Single Cells*, ed. Igakushoin, pp. 283–294. Tokyo: Hongo.

POLIMENI, P. I. (1974). Extracellular space and ionic distribution in rat ventricle. *American Journal of Physiology* **227**, 676–683.

PRESSLER, M. L. (1984). Cable analysis in quiescent and active sheep Purkinje fibres. *Journal of Physiology* **352**, 739–757.

ROBERTS, D. E., HERSH, L. T. & SCHER, A. M. (1979). Influence of cardiac fiber orientation on wavefront voltage, conduction velocity, and tissue resistivity in the dog. *Circulation Research* **44**, 701–712.

RUSH, S., ABILDSKOV, J. A. & MCFEE, R. (1963). Resistivity of body tissue at low frequencies. *Circulation Research* **12**, 40–50.

SOMMER, J. R. (1979). Ultrastructure of cardiac muscle. *Handbook of Physiology – The Cardiovascular System I*, section 2, vol. 1, chap. 5. Bethesda, MD, U.S.A.: American Physiological Society.

SOMMER, J. R. & SCHERER, B. (1985). Geometry of cell and bundle appositions in cardiac muscle: light microscopy. *American Journal of Physiology* **248**, H792–803.

SPACH, M. S., MILLER, W. T., GESELOWITZ, D. B., BARR, R. C., KOOTSEY, J. M. & JOHNSON, E. A. (1981). The discontinuous nature of propagation in normal canine cardiac muscle. Evidence for recurrent discontinuities of intracellular resistance that affects the membrane currents. *Circulation Research* **48**, 39–54.

SUENSON, M. (1985). Interaction between ventricular cells during the early part of excitation in the ferret heart. *Acta physiologica scandinavica* **125**, 81–90.

TILLE, J. (1966). Electrotonic interaction between muscle fibers in the rabbit ventricle. *Journal of General Physiology* **50**, 189–202.

TRANUM-JENSEN, J. & JANSE, M. J. (1982). Fine structural identification of individual cells subjected to microelectrode recording in perfused cardiac preparations. *Journal of Molecular and Cellular Cardiology* **14**, 233–247.

VAN DEN BOS, G. C. & DE JANG-STRAKOVA, Z. (1982). Morphometric measurement of interstitial space in Langendorff perfused rat hearts. *Journal of Physiology* **328**, 69*P*.

VANDER ARK, C. R. & REYNOLDS, E. W. (1970). An experimental study of propagated electrical activity in the canine heart. *Circulation Research* **26**, 451–460.

VEENSTRA, R. D., JOYNER, R. W. & RAWLING, D. A. (1984). Purkinje and ventricular activation sequences of canine papillary muscle. Effects of quinidine and calcium on the Purkinje–ventricular conduction delay. *Circulation Research* **54**, 500–515.

VOGEL, M. W., APSTEIN, C. S., BRIGGS, L. L., GAASCH, W. H. & AHN, J. (1982). Acute alterations in left ventricular diastolic chamber stiffness. Role of the 'erectile' effect of coronary arterial pressure and flow in normal and damaged hearts. *Circulation Research* **51**, 465–478.

WEIDMANN, S. (1952). The electrical constants of Purkinje fibres. *Journal of Physiology* **118**, 348–360.

WEIDMANN, S. (1966). The diffusion of radiopotassium across intercalated disks of mammalian cardiac muscle. *Journal of Physiology* **187**, 323–342.

WEIDMANN, S. (1970). Electrical constants of trabecular muscle from mammalian heart. *Journal of Physiology* **210**, 1041–1054.

WOJTCZAK, J. (1979). Contractures and increase in internal longitudinal resistance of cow ventricular muscle induced by hypoxia. *Circulation Research* **44**, 88–95.